



PERGAMON

Available online at www.sciencedirect.com

SCIENCE @ DIRECT®

Scripta Materialia 49 (2003) 563–569



www.actamat-journals.com

Reactive wetting of molten Al on different oriented α -Al₂O₃ single crystals at high temperatures

Ping Shen^{*}, Hidetoshi Fujii, Taihei Matsumoto, Kiyoshi Nogi

Joining and Welding Research Institute, Osaka University, 11-1 Mihogaoka, Ibaraki, Osaka 567-0047, Japan

Received 7 February 2003; received in revised form 28 May 2003; accepted 5 June 2003

Abstract

The reactive wetting of molten Al on three different oriented α -Al₂O₃ single crystals, $R(01\bar{1}2)$, $A(11\bar{2}0)$ and $C(0001)$, was investigated by an improved sessile drop method at temperatures between 1350 and 1500 °C in a reduced Ar–3%H₂ atmosphere. The wettability is in the order of $R > A > C$. The spreading is reaction-limited and the rate is dominated by the change in the solid–liquid interfacial free energy per unit time.

© 2003 Acta Materialia Inc. Published by Elsevier Ltd. All rights reserved.

Keywords: Wetting; Al; Kinetics; Substrate orientation

1. Introduction

The wetting/spreading of a metal droplet on a smooth solid surface is important for many diverse technologies such as brazing, lubrication and composite infiltration [1]. A fundamental understanding of the wetting/spreading kinetics is essential for process control in related industrial applications. In non-reactive systems, the wetting is controlled by the viscous flow and the equilibrium can be rapidly achieved in times on the order of 10^{-4} – 10^{-1} s. In reactive systems, however, the wetting is interactively coupled with the reaction and the time needed to reach a steady contact angle is usually in the range of 10^{-1} – 10^4 s [2,3].

Two limiting cases in reactive wetting, depending on the rate of the chemical reaction at the triple

line compared to the rate of the reactive solute diffusion from the drop bulk to the triple line, have been identified by Eustathopoulos, Mortensen and their co-workers [2–10]. For systems exhibiting relatively sluggish reaction kinetics, the diffusion of the solute to the triple line is comparatively rapid (or non-existent when the droplet is made of a pure reactive metal). In this case, if the reaction does not significantly change the droplet composition and if a steady configuration is established at the triple junction, the spreading is *reaction-limited* and the triple line velocity is constant with time [2,4],

$$R_t - R_0 = Kt \quad (1)$$

where R_t and R_0 are the droplet base radii at times t and 0, respectively, and K is a system constant, independent of the droplet volume V_d . For systems exhibiting a rapid reaction rate, the solute diffusion is rate-limiting as the contact angle continuously decreases, leading to a reduction in the

^{*} Corresponding author. Tel./fax: +81-668798663.

E-mail address: shenping@jwri.osaka-u.ac.jp (P. Shen).

diffusion field. As a result, the spreading is *diffusion-limited* and can be characterized by [2,8]

$$R_t^4 - R_0^4 = K' V_d t \quad (2)$$

Among the metal–ceramic systems, Al/Al₂O₃ is an intriguing system and the wettability of α -Al₂O₃ by molten Al has been extensively studied [11–19]. However, few specific investigations exist about the wetting/spreading kinetics even though a continuous decrease in the contact angle with time has been observed [14–19]. On the other hand, little information is provided on the effect of substrate anisotropy. In this context, this article represents just such a study.

2. Experimental procedure

Wetting experiments were performed using an improved sessile drop method described in more detail in Ref. [20]. The substrates were high-purity (99.99%) α -Al₂O₃ single crystals, *R*(01 $\bar{1}$ 2), *A*(11 $\bar{2}$ 0) and *C*(0001) (hereafter designated only by the letters *R*, *A* and *C*, respectively) with a surface roughness of less than 1 Å and a crystallographic orientation error of $\pm 0.3^\circ$. The Al specimens were in the form of a wire segment with a purity of 99.99%.

Before the experiments, the samples were ultrasonically cleaned in acetone. The α -Al₂O₃ substrates were placed horizontally in the chamber while the Al segments were placed in the dropping device outside the chamber. The chamber was first evacuated to about 5×10^{-4} Pa at room temperature and then heated to the desired experimental temperature. After the temperature was reached, the chamber was purged with a purified Ar–3% H₂ gas to a pressure of about 0.11 MPa. The Al segment was inserted into the bottom of the alumina tube after the temperature and the atmosphere had stabilized. Molten Al was then forced from a small hole at the bottom of the alumina tube and dropped onto the α -Al₂O₃ substrate by a gradual decrease in the pressure inside the chamber, which creates a small pressure difference between the chamber and the alumina tube. At the same time, the initial surface oxide, if still present, was mechanically removed.

As soon as the molten Al came into contact with the α -Al₂O₃ substrate, a photo was taken and defined as the drop profile at zero time. The captured photographs were analyzed in a computer with automatic image processing programs, in which the contact angle, surface tension and density could be calculated all at once. The drop base diameter/radius, which is a common parameter for the assessment of the movement of the triple line, was directly measured from the drop profiles at a magnification of about 30 times.

3. Results

Fig. 1 shows the variations in contact angle with time for molten Al on the *R*, *A* and *C* α -Al₂O₃ single crystals. The contact angles continuously decrease during the isothermal dwells. The rate of the decrease significantly increases with temperature. However, the angles in the first several tens of seconds, typically no more than 30 s, (see small figures with a logarithmic time scale) do not have a remarkable change with both the temperature and time. On the other hand, they differ rather significantly with the substrate orientation, especially for the *C* face compared with the *R* and *A* faces. Such results are completely different from those reported by Ownby et al. [19], in which the contact angle was concluded to be essentially independent of the crystallographic orientation of the α -Al₂O₃ substrates while the initial angles considerably varied with the temperature. The distinct wettability dependency on the α -Al₂O₃ substrate orientation is possibly related to the different furnace atmosphere, mainly the percent of hydrogen, used in our experiments (Ar–3% H₂) as compared to that in Ownby et al.'s. In the latter, a highly reducing H₂(–He) atmosphere was employed. According to some recently published reports [21–24], H₂ and/or water vapor may change an aluminum-terminated *C*-face α -Al₂O₃ surface to an oxygen-terminated structure, which can lead to a significant improvement on wettability [25] and hence a finally negligible difference in comparison to that of the *R* and *A* faces.

Corresponding to Fig. 1, Fig. 2 shows the variations in the relative base radius, R_t/R_0 with time t .

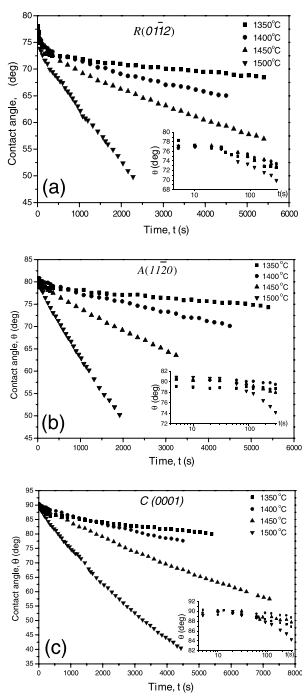


Fig. 1. Variations in contact angle with time during the isothermal dwells for molten Al on the R (a), A (b) and C (c) α -Al₂O₃ substrates.

The R_0 is the drop base radius at 30 s. The results show a well-developed linear relationship between R_t/R_0 and t during the isothermal dwells except for the initial short periods for molten Al on all the R, A and C α -Al₂O₃ single crystals at all the experimental temperatures

$$R_t/R_0 = C_1 + k_1 t \quad (3)$$

The values of the coefficients, C_1 and k_1 are listed in Table 1. Since the values of C_1 are close to 1, it yields an expression similar to Eq. (1), indicating

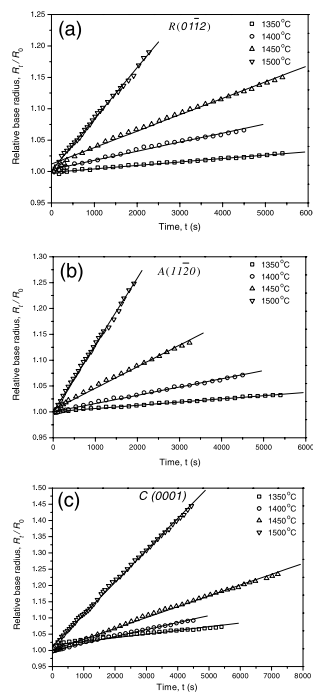


Fig. 2. Variations in the relative base radius with time during the isothermal dwells for molten Al on the R (a), A (b) and C (c) α -Al₂O₃ substrates.

that the spreading in the Al/ α -Al₂O₃ system at high temperatures is *reaction-limited*.

Note that the coefficient k_1 in Eq. (3) represents the spreading rate, hence the data in Table 1 show that the spreading rate depends not only on the temperature but also on the substrate orientation. An increase in the temperature of about 150 °C will lead to an increase in the spreading rate of more than one order. On the other hand, at relatively low temperatures ($T \leq 1400$ °C), the spreading of the molten Al on the C face is the fastest, whereas at high temperatures ($T > 1400$ °C), the

Table 1
Coefficients of C_1 and k_1 in Eq. (3) obtained from linear fit of the data in Fig. 2

Temperature (°)	R		A		C	
	C_1	k_1 (s ⁻¹)	C_1	k_1 (s ⁻¹)	C_1	k_1 (s ⁻¹)
1350	1.00	5.47E-6	1.00	6.22E-6	1.02	9.09E-6
1400	1.00	1.55E-5	1.00	1.60E-5	1.00	2.14E-5
1450	1.01	2.61E-5	1.00	4.17E-5	1.00	3.34E-5
1500	1.00	8.18E-5	1.00	1.30E-4	1.01	9.84E-5

spreading on the *A* face tends to be the fastest. The magnitude of the increase for the *A* face is much more significant than that for the *R* and *C* faces. The different spreading rates on the different faces of the α -Al₂O₃ crystals indicate that the substrate orientation affects not only the wettability but also the wetting progress.

4. Discussion

As indicated in Fig. 1, the wetting/spreading process in the Al/ α -Al₂O₃ system, from a simple point of view, might be divided into two stages. The first stage is very short, typically no more than 30 s and can be characterized by the very rapid wetting (for the *R* and *A* faces) or near wetting (for the *C* face) under the driving force of balancing the interfacial tensions. A *transient static equilibrium* may exist in this stage since the contact angles remain almost constant [26]. These angles are also the true contact angles because the contact surface is smooth; while after a relatively long dwell time, the surface, especially at the triple junction, is no longer smooth due to the α -Al₂O₃ dissolution and reaction with the molten Al, therefore, the angles measured in the later periods, in a strict sense, are no longer the true contact angles as described by Young's equation but the apparent ones. The second stage is a long and progressive spreading stage, mainly characterized by a constant spreading rate with a continuous decrease in the contact angle and increase in the drop base diameter/radius as the α -Al₂O₃ substrate progressively reacts with the molten Al. The linear spreading in the Al/ α -Al₂O₃ system seems similar to that in other *reaction-limited* systems such as Al/C [4,5], CuSi/SiC [6] and CuSi/C_v [7]. However, a major difference is that the reaction product at the Al/ α -Al₂O₃ interface is a gas phase (Al₂O) which can easily run away either directly from the triple line or through the liquid bulk. As a consequence, the contact phases at the liquid–solid interface are permanently the molten Al and solid α -Al₂O₃ and the reaction between them will never end as long as the partial pressure of the Al₂O gas in the atmosphere does not reach its equilibrium value, leading to an inaccessible steady equilibrium angle even after

isothermal dwells for 8 h as demonstrated in Ownby et al.'s experiments [19]. Whereas, in most reactive wetting systems, the substrate dissolves in the liquid and usually forms novel compounds (different from the substrate phase), initially as discrete crystals nucleating on the preferred sites at the solid–liquid interface and later growing into a continuous layer of the reaction product(s). Such reactions yield one or more interfaces rather than a single one as in the Al/ α -Al₂O₃ system, and the final static wetting equilibrium is established at the newly formed liquid–solid interface after either a short or long wetting period. As a result, the equilibrium contact angles in these systems are usually represented by the final static wetting angles.

Here, we assume the first stage in the Al/ α -Al₂O₃ system as a transient static equilibrium stage and the contact angles in this stage, or more definitely, at the time of about 30 s as the equilibrium angles (θ_0). Table 2 gives their values (they may have some errors in comparison to the true equilibrium contact angles). Note that they vary only slightly with the temperature but relatively significantly with the substrate orientation. The reasons for the dependence of the wettability on the substrate orientation have been presented elsewhere [27].

The static equilibrium is broken and the triple line starts to move when the chemical reaction between the molten Al and α -Al₂O₃ substrate occurs and causes a reduction in the solid–liquid interfacial free energy, σ_{sl} ,

$$\sigma_{sl} = \sigma_{sl}^0 + \Delta\sigma(t) \quad (4)$$

where σ_{sl}^0 is the initial equilibrium solid–liquid interfacial free energy and $\Delta\sigma(t)$ is the change in the solid–liquid interfacial free energy. At this time, a

Table 2
Assumed equilibrium contact angles for the molten Al on the *R*, *A* and *C* α -Al₂O₃ crystals at temperatures ranging from 1350 to 1500 °C

α -Al ₂ O ₃ face	Equilibrium contact angles, θ_0 (°)			
	1350 °C	1400 °C	1450 °C	1500 °C
<i>R</i>	77	77	77	77
<i>A</i>	79	80	80	81
<i>C</i>	89	90	90	89

driving force for the initiation of the spreading is produced. Assuming that the solid–vapor and liquid–vapor interfacial free energies, σ_{sv} and σ_{lv} , do not change with time, the substrate surface is flat and the viscous resistance can be neglected, the driving force can be expressed by

$$F(t) = \sigma_{sv} - (\sigma_{sl}^0 + \Delta\sigma(t)) - \sigma_{lv} \cos \theta_t \quad (5a)$$

or

$$F(t) = -\Delta\sigma(t) + \sigma_{lv}(\cos \theta_0 - \cos \theta_t) \quad (5b)$$

As the reaction progresses, the spreading goes into a *dynamic equilibrium stage* [26,28] since the spreading rate is constant as reflected in Fig. 2, which also means that the driving force decreases again to zero, otherwise, the spreading rate will not be constant but further increase. It is conceivable that from the static equilibrium stage to the dynamic equilibrium stage, a non-equilibrium transition stage must be experienced, in which the spreading rate is accelerated to the constant value under the action of the driving force. In this sense, the entire wetting/spreading process may consist of three stages rather than two, i.e., (i) a transient static equilibrium stage, (ii) a non-equilibrium transition stage, and (iii) a dynamic equilibrium spreading stage. However, a detailed analysis on the non-equilibrium transition stage is not presented in this article.

As the dynamic equilibrium is reached, the driving force, $F = 0$. Therefore, from Eq. (5b), we obtain

$$\Delta\sigma(t) = \sigma_{lv}(\cos \theta_0 - \cos \theta_t) \quad (6)$$

Considering that the spreading kinetics can also be reflected from the variations in the contact angle (θ_t) with time (t), Fig. 3 shows the plots of $\ln(\theta_t/\theta_0)$ vs. time (t) at various temperatures. It seems that

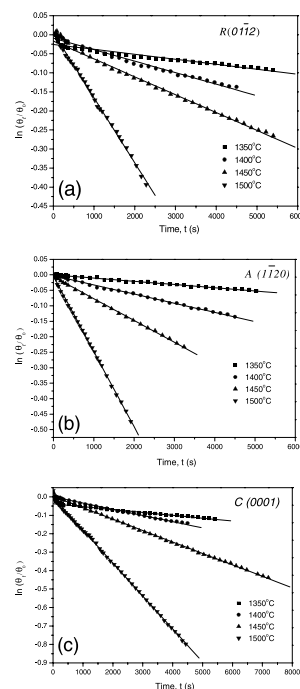


Fig. 3. Plots of $\ln(\theta_t/\theta_0)$ vs. t for the molten Al on the R (a), A (b) and C (c) α - Al_2O_3 substrates at various temperatures.

the time-dependent contact angles fit well with the following linear equation

$$\ln(\theta_t/\theta_0) = k_2t + C_2 \quad (7)$$

where k_2 and C_2 are coefficients and their values are listed in Table 3. Note that the values of C_2 are close to zero, thus Eq. (7) can be simplified as

$$\ln(\theta_t/\theta_0) = k_2t \quad (8)$$

or written as

$$\theta_t = \theta_0 e^{k_2t} \quad (9)$$

Table 3

Coefficients of C_2 and k_2 in Eq. (7) obtained from linear fit of the data in Fig. 3

Temperature (°)	R		A		C	
	C_2	k_2 (s ⁻¹)	C_2	k_2 (s ⁻¹)	C_2	k_2 (s ⁻¹)
1350	-0.03	-1.15E-5	0	-1.04E-5	-0.04	-1.62E-5
1400	-0.01	-3.02E-5	0	-2.97E-5	0	-3.31E-5
1450	-0.01	-4.96E-5	-0.01	-7.06E-5	0	-6.23E-5
1500	0.01	-1.71E-4	0.01	-2.43E-4	0.01	-1.76E-4

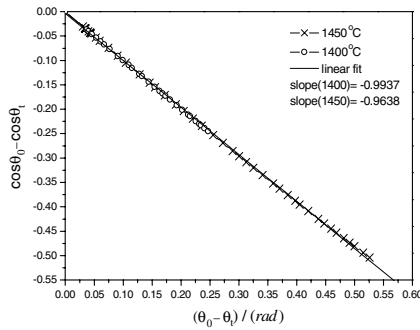


Fig. 4. Plot of $(\cos \theta_0 - \cos \theta_t)$ vs. $(\theta_0 - \theta_t)/\text{rad}$ for the molten Al on the C $\alpha\text{-Al}_2\text{O}_3$ substrates at the temperatures of 1400 and 1450 °C, showing that $(\cos \theta_0 - \cos \theta_t) \approx -(\theta_0 - \theta_t)/(\text{rad})$, where rad is the unit of θ (radian).

i.e., the time-dependent contact angle exhibits an exponential decay law for the molten Al on all the $\alpha\text{-Al}_2\text{O}_3$ substrates.

Furthermore, if we only consider a relatively short spreading period, Eq. (9) is approximated to

$$\theta_t \approx \theta_0 + kt \quad (k = k_2\theta_0) \quad (10)$$

which shows a linear relationship between the dynamic angle and time.

Since $(\cos \theta_0 - \cos \theta_t) \approx -(\theta_0 - \theta_t)/(\text{rad})$, (as an illustration, Fig. 4 shows the plot of $(\cos \theta_0 - \cos \theta_t)$ vs. $(\theta_0 - \theta_t)/(\text{rad})$ and the linear fit results), we can further derive from Eq. (6)

$$\Delta\sigma(t) \approx -\sigma_{\text{LV}}(\theta_0 - \theta_t)/(\text{rad}) \approx \sigma_{\text{LV}}(k/\text{rad})t \quad (11)$$

or

$$\Delta\sigma_t = \Delta\sigma(t)/t \approx k'\sigma_{\text{LV}} \quad (k' = k/\text{rad}) \quad (12)$$

i.e., when a dynamic equilibrium of spreading is established, the change in the solid–liquid interfacial free energy per unit time ($\Delta\sigma_t$, $\text{N m}^{-1} \text{s}^{-1}$) is approximately equal to the product of the spreading rate (k' , s^{-1}) and the liquid–vapor interfacial free energy (σ_{LV} , N m^{-1}).

5. Conclusions

The initial equilibrium contact angles of the molten Al on the $\alpha\text{-Al}_2\text{O}_3$ single crystals do not significantly change with the temperature but vary relatively significantly with the substrate orienta-

tion at high temperatures between 1350 and 1500 °C in a reduced Ar–3% H_2 atmosphere. The wettability of the three faces of the $\alpha\text{-Al}_2\text{O}_3$ single crystals is in the order of $R > A > C$.

The high-temperature reactive wetting kinetics, from a strict point of view, consists of three stages: (i) the transient static equilibrium stage, (ii) the non-equilibrium transition stage, and (iii) the dynamic equilibrium spreading stage. Both of the first two stages are very short while the third one can experience a long time. In stage (iii), the spreading is reaction-limited, characterized not only by a linear relationship of the drop base radius (R_t) vs. time (t), $R_t/R_0 = 1 + k_1t$, but also by an exponential decay law of the dynamic contact angle (θ_t) vs. time (t), $\theta_t = \theta_0 \exp(k_2t)$. Most importantly, the spreading rate (k') is essentially dominated by the change in the solid–liquid interfacial free energy per unit time ($\Delta\sigma_t$).

Acknowledgements

This work is supported by the NEDO International Joint Research Grant and the 21st Century COE Program.

References

- [1] Ambrose JC, Nicholas MG, Stoneham AM. *Acta Metall Mater* 1993;41:2395.
- [2] Eustathopoulos N. *Acta Mater* 1998;46:2319.
- [3] Mortensen A, Drevet B, Eustathopoulos N. *Scr Mater* 1997;36:645.
- [4] Landry K, Eustathopoulos N. *Acta Mater* 1996;44:3923.
- [5] Landry K, Kalogeropoulou S, Eustathopoulos N. *Mater Sci Eng* 1998;A254:99.
- [6] Dezellus O, Hodaj F, Barbier JN, Rado C, Eustathopoulos N. *Acta Mater* 2002;50:979.
- [7] Landry K, Rado C, Eustathopoulos N. *Metall Mater Trans A* 1996;27A:318.
- [8] Mortensen A, Drevet B, Eustathopoulos N. *Scr Mater* 2001;45:953.
- [9] Voitovitch R, Mortensen A, Hodaj F, Eustathopoulos N. *Acta Mater* 1999;47:1117.
- [10] Dezellus O, Hodaj F, Barbier JN, Rado C, Eustathopoulos N. *Scr Mater* 2001;44:2543.
- [11] Laurent V, Chatain D, Chatillon C, Eustathopoulos N. *Acta Metall* 1988;36:1797.

- [12] John H, Hansner H. *J Mater Sci Lett* 1986;5:549.
- [13] Wang D-J, Wu S-T. *Acta Metall Mater* 1994;42:4029.
- [14] Brennan JJ, Pask JA. *J Am Ceram Soc* 1968;51:569.
- [15] Jung W, Song H, Pask SW, Kim D-Y. *Metall Mater Trans B* 1996;27B:51.
- [16] Levi G, Kaplan WD. *Acta Mater* 2002;50:75.
- [17] Carnahan RD, Johnston TL, Li CH. *J Am Ceram Soc* 1958;41:343.
- [18] Champion JA, Keen BJ, Sillwood JM. *J Mater Sci* 1969;4:39.
- [19] Ownby PD, Li Ke Wen K, Weirauch Jr DA. *J Am Ceram Soc* 1991;74:1275.
- [20] Shen P, Fujii H, Matsumoto T, Nogi K. *Scr Mater* 2003;48:779.
- [21] Liu P, Kendelewicz T, Brown Jr GE, Nelson EJ, Chambers SA. *Surf Sci* 1998;417:53.
- [22] Eng PJ, Trainor TP, Brown Jr GE, Waychunas GA, Newville M, Sutton SR, Rivers ML. *Science* 2000;288(12):1029.
- [23] Wang XG, Chaka A, Scheffler M. *Phys Rev Lett* 2000;84:3650.
- [24] Felice RD, Northrup JE. *Phys Rev B* 1999;60:16287.
- [25] Zhang W, Smith JR. *Phys Rev Lett* 2000;85:3225.
- [26] Nakae H, Fujii H, Sato K. *Mater Trans JIM* 1992;33:400.
- [27] Shen P, Fujii H, Matsumoto T, Nogi K. *Acta Mater*, in press.
- [28] Yoshimi N, Nakae H, Fujii H. *Mater Trans JIM* 1990;33:141.